JOC Article
pubs.acs.org/joc

# Charged Tags as Probes for Analyzing Organometallic Intermediates and Monitoring Cross-Coupling Reactions by Electrospray-Ionization Mass Spectrometry

Matthias A. Schade, Julia E. Fleckenstein, Paul Knochel, and Konrad Koszinowski*

*Department Chemie, Ludwig-Maximilians-Universität München, Butenandtstr. 5-13, 81377 München, Germany*

*konrad.koszinowski@cup.uni-muenchen*

*Received July 7, 2010*

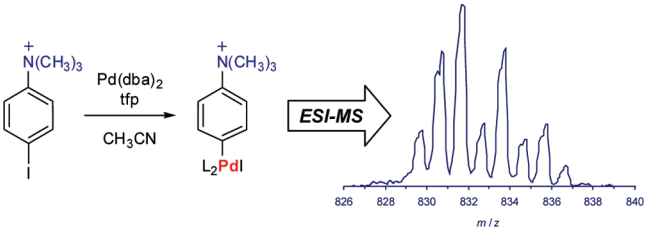


Organic iodides bearing a cationic quaternary ammonium group at a remote position react with zerovalent Pd complexes, Zn, or In leading to a C−I bond insertion. The resulting charge-tagged organometallics can be detected by electrospray-ionization mass spectrometry, which provides detailed information on their stoichiometry, oxidation state, and coordination sphere. The properties of the observed organopalladium and -zinc intermediates largely agree with previous findings, whereas the organoindium species show a surprisingly high tendency to form ate complexes. Magnesium also undergoes insertion into the C−I bond of the charge-tagged organic iodides, but instead of the expected organomagnesium intermediates only the corresponding hydrolysis products could be detected in the diluted solutions. Electrospray-ionization mass spectrometry can also be used to study the reactivity of the charge-tagged species, as was demonstrated for a Pd-catalyzed Negishi cross-coupling reaction. The presented approach permits a straightforward identification of the rate-limiting step and the determination of the corresponding second-order rate constant.

## Introduction

The majority of elements in the periodic table are metals, virtually all of which can bind to carbon. The resulting manifold of organometallics gives rise to an enormous diversity in terms of electronic properties, coordination geometries, and aggregation states. This diversity in turn leads to various reactivity patterns and offers tremendous opportunities for synthesis and catalysis. However, elucidating the mechanism of many synthetically or catalytically useful reactions involving organometallics is rather difficult. In particular, the ability of metal centers to switch between different oxidation or coordination states and to engage in dynamic equilibria can dramatically complicate the situation. Several analytical techniques have been used to address this problem. Highly detailed and valuable structural information is given by X-ray crystallography. However, this method does not provide direct insight into the behavior of reactive intermediates in solution. In contrast, spectroscopic techniques can directly probe dissolved organometallic species. While NMR, IR, UV−vis, and X-ray spectroscopy are suitable for the identification of reactive organometallic intermediates, the information obtained by these methods is not always sufficient for a full characterization of the system under investigation. Particularly, the distinction between different coordination and aggregation states can be challenging.

An alternative approach, which may help to overcome these problems by providing unambiguous stoichiometric information, relies on electrospray-ionization (ESI) mass spectrometry.[1] This method permits the transfer of ions from

(1) Yamashita, M.; Fenn, J. B. *J. Phys. Chem.* **1984**, *88*, 4451–4459.



Published on Web 09/13/2010 DOI: 10.1021/jo101337a

solution into the gas phase, thus allowing the sampling of dissolved charged organometallics *in situ*. It is therefore not surprising that ESI mass spectrometry has been applied to the analysis of numerous different organometallic systems.[2] The successful detection of various charged organometallics, including rather labile ones,[2,3] is consistent with the commonly accepted view that ESI constitutes a relatively "soft" ionization technique, which transfers only limited amounts of energy into the probed ions and does not significantly change their nature.[4] This assumption forms the basis on which properties of the solution-phase system are deduced from gas-phase measurements.

Unlike spectroscopic techniques, ESI mass spectrometry exclusively detects charged species. This feature can be advantageous if ionic systems shall be probed selectively. In most cases, however, the restriction to charged species forms a substantial drawback because neutral organometallics usually prevail over their ionized counterparts. While the fraction of ionized species may be increased by additives that lead to protonation, deprotonation, or complexation,[2a] these reactions can possibly change the nature of the organometallic system under investigation. For instance, protonation will obviously adversely affect organometallics sensitive to hydrolysis. In other cases, the use of additives may have more subtle effects and can thus lead to less conspicuous artifacts.

A potentially better approach pioneered by Colton and Traeger[5] and the groups of Dyson[6] and Chen[2c,7] uses covalently attached charged tags to make neutral organometallics amenable to ESI mass spectrometry. Provided that the charged tags have only low tendencies to form ion pairs with the counterions in the chosen solvent, almost the complete population of neutral organometallics can thus be ionized. Commonly employed tags are quaternary ammonium cations[2,5,7−9] and sulfonate anions.[6,10] In these ions, the charge is spread over several atoms, which not only reduces their propensity to ion pairing but also minimizes possible interactions with the metal center and unwanted changes in reactivity. Most of the examples reported so far bear a charged tag linked to coordinating ligands,[11] such as phosphines[6,7a,7c,9,10] or carbenes.[7d] Obviously, this strategy is particularly suited for probing transition metal complexes, whereas it cannot be applied to the detection of main-group organometallics that do not bear coordinating ligands.

Alternatively, the charged tag can be directly incorporated into an organyl moiety covalently bound to the metal center.[7b,12,13] This tagging scheme not only enables the analysis of systems lacking coordinating ligands but also lends itself to the analysis of coupling reactions that transfer the organyl moiety with the charged tag and thus ensure straightforward product identification. Herein, we show that organometallics with covalently bound charged tags can be accessed by insertion of zerovalent metals [M] into charge-tagged organic iodides, such as (*p*-iodophenyl)-trimethylammonium iodide ($[\mathbf{ArI}]^+I^-$) and triethyl-(4-iodobutyl)-ammonium iodide ($[\mathbf{RI}]^+I^-$), eqs 1 and 2.[14]

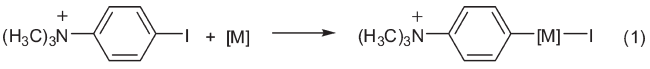


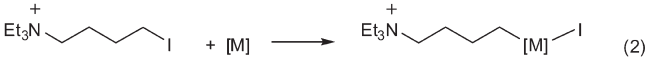


To prove the generality of this strategy, we tested its feasibility for insertion reactions of metals of widely differing reactivity, namely, of Pd, Zn, Mg, and In (for the latter, eqs 1 and 2 do not apply in the form given because the insertion products supposedly correspond to In(+3) species).[15] In all cases, we analyzed the solutions of the reaction products by ESI mass spectrometry and compare the obtained results with available data for the related untagged systems. Moreover, we also demonstrated that ESI mass spectrometry can be used for monitoring cross-coupling reactions of charge-tagged substrates and analyzing their kinetics.

## Results and Discussion

**Organopalladium Species.** Because of the immense importance of Pd catalysis in modern organic synthesis, the mechanisms of Pd-mediated cross-coupling and Heck reactions have been investigated in great detail.[16] The first step in the catalytic cycle of these reactions typically is the insertion of a Pd(0) species into the Ar−X bond of substitued arenes

(2) For selected reviews, see: (a) Traeger, J. C. *Int. J. Mass Spectrom.* **2000**, *200*, 387–401. (b) Plattner, D. A. *Int. J. Mass Spectrom.* **2001**, *207*, 125–144. (c) Chen, P. *Angew. Chem.* **2003**, *115*, 2938–2954; *Angew. Chem., Int. Ed.* **2003**, *42*, 2832−2847. (d) Santos, L. S.; Knaack, L.; Metzger, J. O. *Int. J. Mass Spectrom.* **2005**, *246*, 84–104. (e) Henderson, W.; McIndoe, J. S. *Mass Spectrometry of Inorganic, Coordination and Organometallic Compounds: Tools, Techniques, Tips*; Wiley: Chichester, 2005; pp 175−219. (f) Müller, C. A.; Markert, C.; Teichert, A. M.; Pfaltz, A. *Chem. Commun.* **2009**, 1607–1618. (g) Roglans, A.; Pla-Quintana, A. In *Reactive Intermediates: MS Investigations in Solution*; Santos, L. S., Ed.; Wiley-VCH: Weinheim, 2009; pp 229−276.

(3) (a) Hammad, L. A.; Gerdes, G.; Chen, P. *Organometallics* **2005**, *24*, 1907–1913. (b) Moret, M.-E.; Chen, P. *Organometallics* **2007**, *26*, 1523–1530.

(4) Cole, R. B. *J. Mass Spectrom.* **2000**, *35*, 763–772.

(5) (a) Colton, R.; Traeger, J. C. *Inorg. Chim. Acta* **1992**, *201*, 153–155. (b) Ahmed, I.; Bond, A. M.; Colton, R.; Jurcevic, M.; Traeger, J. C.; Walter, J. N. *J. Organomet. Chem.* **1993**, *447*, 59–65.

(6) Bryce, D. J. F.; Dyson, P. J.; Nicholson, B. K.; Parker, D. G. *Polyhedron* **1998**, *17*, 2899–2905.

(7) (a) Hinderling, C.; Adlhart, C.; Chen, P. *Angew. Chem.* **1998**, *110*, 2831–2835; *Angew. Chem., Int. Ed.* **1998**, *37*, 2685−2689. (b) Adlhart, C.; Chen, P. *Helv. Chim. Acta* **2000**, *83*, 2192–2196. (c) Adlhart, C.; Hinderling, C.; Baumann, H.; Chen, P. *J. Am. Chem. Soc.* **2000**, *122*, 8204–8214.

(8) Adlhart, C.; Chen, P. *Helv. Chim. Acta* **2003**, *86*, 941–949.

(9) Dorcier, A.; Dyson, P. J.; Gossens, C.; Rothlisberger, U.; Scopelliti, R.; Tavernelli, I. *Organometallics* **2005**, *24*, 2114–2123.

(10) Basset, J.-M.; Bouchu, D.; Godard, G.; Karamé, I.; Kuntz, E.; Lefebvre, F.; Legagneux, N.; Lucas, C.; Michelet, D.; Tommasino, J. B. *Organometallics* **2008**, *27*, 4300–4309.

(11) For a recent review, see: Chisholm, D. M.; McIndoe, J. S. *Dalton Trans.* **2008**, 3933–3945.

(12) Crawford, E.; Lohr, T.; Leitao, E. M.; Kwok, S.; McIndoe, J. S. *Dalton Trans.* **2009**, 9110–9112.

(13) (a) O'Hair, R. A. J.; Waters, T.; Cao, B. *Angew. Chem.* **2007**, *119*, 7178–7181; *Angew. Chem., Int. Ed.* **2007**, *46*, 7048−7051. (b) Khairallah, G. N.; Yoo, E. J. H.; O'Hair, R. A. J. *Organometallics* **2010**, *29*, 1238–1245.

(14) An analogous insertion reaction of In into a charged-tagged allyl bromide has recently been reported: Koszinowski, K. *J. Am. Chem. Soc.* **2010**, *132*, 6032–6040.

(15) Weidlein, J. *Gmelin Handbook of Inorganic and Organometallic Chemistry: Organoindium Compounds 1*, 8th ed.; Petz, W., Ed.; Springer: Berlin, 1991.

(16) For selected reviews, see: (a) Amatore, C.; Jutand, A. *Acc. Chem. Res.* **2000**, *33*, 314–321. (b) Beletskaya, I. P.; Cheprakov, A. V. *Chem. Rev.* **2000**, *100*, 3009–3066. (c) Littke, A. F.; Fu, G. C. *Angew. Chem.* **2002**, *114*, 4350–4386; *Angew. Chem., Int. Ed.* **2002**, *41*, 4176−4211. (d) Herrmann, W. A.; Öfele, K.; Preysing, D. v.; Schneider, S. K. *J. Organomet. Chem.* **2003**, *687*, 229–248. (e) Farina, V. *Adv. Synth. Catal.* **2004**, *346*, 1553–1582. (f) de Vries, J. G. *Dalton Trans.* **2006**, 421–429. (g) Phan, N. T. S.; van der Sluys, M.; Jones, C. W. *Adv. Synth. Catal.* **2006**, *348*, 609–679.

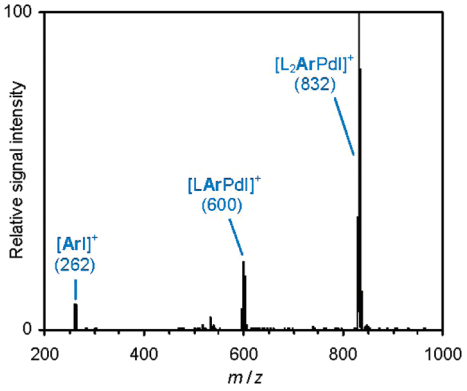


**FIGURE 1.** Positive ion mode ESI mass spectrum of an approximately 0.15 mM solution of the products ($m/z$ ratios of the most abundant isotopologues in brackets) formed upon reaction of Pd(dba)$_2$ with (*p*-iodophenyl)-trimethylammonium iodide ([**ArI**]$^+$I$^-$) and tri(2-furyl)phosphine (L, 2 equiv) in $CH_3CN$ measured with the HCT ion trap.

**SCHEME 1. Insertion of $PdL_2$ (L = ligand) into Ar-X bonds and Consecutive Heterolytic Dissociation**

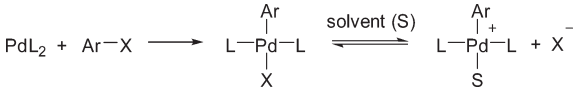


(X = halogen, $OSO_2CF_3$, $N_2^+$, etc). Numerous ESI mass spectrometric studies have provided indirect evidence of these insertion products by detecting related cationic species that form upon heterolytic dissociation of X$^-$ (Scheme 1; in the case of X = $N_2^+$ the dissociation step is very fast and irreversible).[2g,17] Accordingly, most of these studies have focused on Pd insertion into aryl triflates[17a,c,i] and aryl diazonium cations,[17b,d,e,g,h] whose good leaving groups facilitate cationization of the insertion products. In contrast, the use of charge-tagged substrates promises to suspend this limitation and to make possible the direct observation of the insertion products.[18]

We first turned our attention to the reaction of bis(dibenzylideneacetone) palladium (Pd(dba)$_2$)/tri(2-furyl)-phosphine (tfp = L, 2 equiv) with [**ArI**]$^+$I$^-$ (1 equiv) in acetonitrile. Positive ion mode ESI mass spectrometric analysis of the diluted product solution showed relatively small amounts of remaining reactant [**ArI**]$^+$ ($m/z$ 262) as well as mononuclear Pd complexes (Figure 1) that are readily identifiable by their characteristic isotope pattern (Figures S1 and S2, Supporting Information).[19] The base peak corresponds to the insertion product [L$_2$**Ar**PdI]$^+$ ($m/z$ 832 for the most abundant $^{106}$Pd containing isotopologue) whose formation is fully in line with the expected mechanism (Scheme 1).[20] Its identity was also confirmed by fragmentation experiments, which lead to the loss of one tfp ligand (Figures S3 and S4, Supporting Information). To a minor extent, this ligand expulsion apparently also occurs already during the ESI process (in the absence of any extra activation), as the detection of [L**Ar**PdI]$^+$ ($m/z$ 600) in small signal intensity indicates (Figure 1).

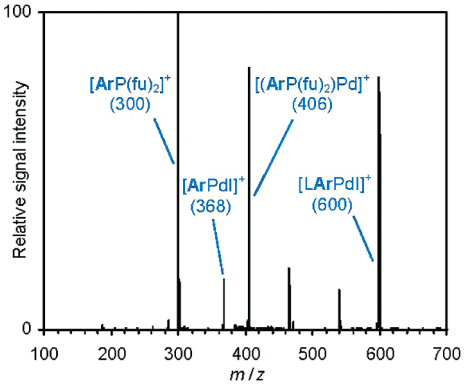


**FIGURE 2.** Mass spectrum of mass-selected [L**Ar**$^{106}$PdI]$^+$ (**Ar** = *p*-trimethylammonium-phenyl, L = tri(2-furyl)phosphine, fu = 2-furyl) and its fragment ions ($m/z$ ratios in brackets) produced upon collision-induced dissociation ($V_{exc}$ = 0.23 V, HCT ion trap). The ions centered at $m/z$ 466 and 541 presumably result from the loss of $fu_2$ and $N(CH_3)_3$, respectively.

Notably, the fragmentation reactions observed for [L**Ar**PdI]$^+$ ($m/z$ 600) not only include simple loss of the tfp ligand but also involve the exchange of a furyl substituent for the charge-tagged **Ar**$^+$ group (Figures 2 and S5, Supporting Information), eqs 3a and 3b.[21]

$$[\mathrm{L}\mathbf{Ar}\mathrm{PdI}]^+ \rightarrow [(\mathbf{Ar}\mathrm{P}(\mathrm{furyl})_2)\mathrm{Pd}]^+ + (\mathrm{furyl})\mathrm{I} \quad (3a)$$

$$\rightarrow [\mathrm{Pd}, (\mathrm{furyl})\mathrm{I}] + [\mathbf{Ar}\mathrm{P}(\mathrm{furyl})_2]^+ \quad (3b)$$

Analogous C−P activations and aryl scrambling reactions have been reported previously for Pd(+2) complexes.[22] The absence of ions indicative of such scrambling reactions in the ESI mass spectrum recorded for the diluted reaction mixture (Figure 1) suggests that these reactions proceed only upon provision of additional energy during the fragmentation experiments.

In a similar manner, the reaction of [**ArI**]$^+$I$^-$ with Pd(PPh$_3$)$_4$ was investigated. In comparison to the experiments employing the tfp ligand, the higher amounts of remaining reactant [**ArI**]$^+$ ($m/z$ 262) point to a slower insertion reaction (Figure 3). This finding is in accordance with the less electron-rich character of

(17) (a) Brown, J. M.; Hii, K. K. *Angew. Chem.* **1996**, *108*, 679–682; *Angew. Chem., Int. Ed. Engl.* **1996**, *35*, 657−659. (b) Masllorens, J.; Moreno-Mañas, M.; Pla-Quintana, A.; Roglans, A. *Org. Lett.* **2003**, *5*, 1559–1561. (c) Jutand, A.; Négri, S. *Organometallics* **2003**, *22*, 4429–4237. (d) Sabino, A. A.; Machado, A. H. L.; Correia, C. R. D.; Eberlin, M. N. *Angew. Chem.* **2004**, *116*, 2568–2572; *Angew. Chem., Int. Ed.* **2004**, *43*, 2514−2518. (e) Pla-Quintana, A.; Roglans, A. *Arkivoc* **2005**, *ix*, 51–62. (f) Santos, L. S.; Rosso, G. B.; Pilli, R. A.; Eberlin, M. N. *J. Org. Chem.* **2007**, *72*, 5809–5912. (g) Masllorens, J.; González, I.; Roglans, A. *Eur. J. Org. Chem.* **2007**, 158–166. (h) Taccardi, N.; Paolillo, R.; Gallo, V.; Mastrorilli, P.; Nobile, C. F.; Räisänen, M.; Repo, T. *Eur. J. Inorg. Chem.* **2007**, 4645–4652. (i) Svennebring, A.; Sjöberg, P. J. R.; Larhed, M.; Nilsson, P. *Tetrahedron* **2008**, *64*, 1808–1812. (j) Lindh, J.; Sävmarker, J.; Nilsson, P.; Sjöberg, P. J. R.; Larhed, M. *Chem.—Eur. J.* **2009**, *15*, 4630–4636. (k) Buarque, C. D.; Pinho, V. D.; Vaz, B. G.; Eberlin, M. N.; da Silva, A. J. M.; Costa, P. R. R. *J. Organomet. Chem.* **2010**, *695*, 2062–2067.

(18) For an early report of the observation of a protonated intact insertion product by ESI mass spectrometry, see: Aliprantis, A. O.; Canary, J. W. *J. Am. Chem. Soc.* **1994**, *116*, 6985–6986.

(19) Theoretical isotope patterns can be conveniently calculated with web-based resources, such as http://yanjunhua.tripod.com/pattern.htm.

(20) Note that the mass spectrometric results do not determine the stereochemistry of this and other complexes but that *trans* geometries appear likely on the basis of their generally accepted higher stability; see, e.g., ref 16b.

(21) Note that only the ionic fragments are directly observable, whereas their neutral counterparts must be inferred.

(22) (a) Herrmann, W. A.; Brossmer, C.; Priermeier, T.; Öfele, K. *J. Organomet. Chem.* **1994**, *481*, 97–108. (b) Herrmann, W. A.; Brossmer, C.; Öfele, K.; Beller, M.; Fischer, H. *J. Organomet. Chem.* **1995**, *491*, C1–C4.

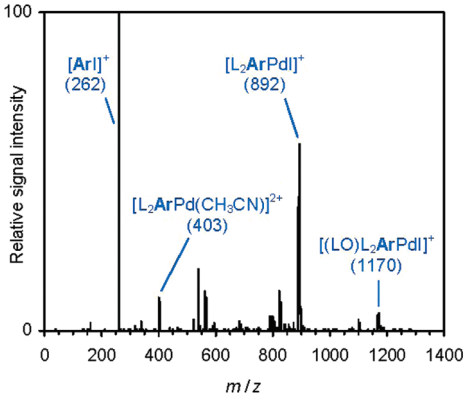


**FIGURE 3.** Positive ion mode ESI mass spectrum of an approximately 0.15 mM solution of the products ($m/z$ ratios of the most abundant isotopologues in brackets) formed upon reaction of Pd($PPh_3$)$_4$ with (*p*-iodophenyl)-trimethylammonium iodide ([**ArI**]$^+$I$^-$) in $CH_3CN$ (L = $PPh_3$). The ion at $m/z$ = 540 corresponds to [(LO)-**ArI**]$^+$; those at $m/z$ 562 and 824 are assigned to [L$_n$**Ar**$^{106}$Pd(OAc)]$^+$ ($n$ = 1 and 2, respectively).

the $PPh_3$ ligand, which is known to slow down oxidative additions to the Pd center.[23] Besides the expected insertion product [L$_2$**Ar**PdI]$^+$ ($m/z$ 892, L = $PPh_3$, Figure S6, Supporting Information), several related Pd(+2) complexes were observed. Among these, the [L$_n$**Ar**Pd(OAc)]$^+$ species, $n$ = 1 and 2 ($m/z$ 562 and 824, respectively) probably resulted from an exchange of the iodo ligand for acetate (being present as a contamination), while the [(LO)L$_2$**Ar**PdI]$^+$ complex ($m/z$ 1170) corresponds to the adduct of the initial insertion product with triphenylphosphine oxide. The latter can be easily generated by oxidation of $PPh_3$ by traces of oxygen and also formed an adduct with residual reactant [**ArI**]$^+$ (Figure 3).

Fragmentation experiments of the Pd-containing complexes (Figures S7−S12, Supporting Information) showed simple ligand losses and C−P activation reactions analogous to those observed for the related [(tfp)**Ar**PdI]$^+$ species (see above), eqs 4a and 4b.

$$[L_2\mathbf{Ar}PdI]^+ \rightarrow [(\mathbf{Ar}PPh_2)Pd]^+ + PhI + L \quad (4a)$$

$$\rightarrow [Pd,\ L,\ PhI] + [\mathbf{Ar}PPh_2]^+ \quad (4b)$$

In addition, C−H bond activations apparently occur for the acetate-containing complexes [L$_n$**Ar**Pd(OAc)]$^+$ (Figures S9 and S10, Supporting Information), eq 5.

$$[L_n\mathbf{Ar}Pd(OAc)]^+ \rightarrow [L\mathbf{Ar}Pd - H]^+ + HOAc + (n-1)L,\quad n = 1 \text{ and } 2 \quad (5)$$

A completely analogous gas-phase fragmentation reaction has been observed for [L$_2$Pd(OAc)]$^+$.[24] In this case, the hydrogen atom transferred to the expelled acetate moiety presumably originated from the ortho position of a phenyl substituent in the $PPh_3$ ligand. Most likely, the HOAc elimination from the [L$_n$**Ar**Pd(OAc)]$^+$ complexes follows a similar mechanism.

(23) Martin, R.; Buchwald, S. L. *Acc. Chem. Res.* **2008**, *41*, 1461–1473.
(24) Qian, R.; Guo, H.; Liao, Y.; Wang, H.; Zhang, X.; Guo, Y. *Rapid Commun. Mass Spectrom.* **2006**, *20*, 589–594.

All of the so far discussed ions detected upon ESI of the diluted reaction mixture of Pd($PPh_3$)$_4$ and [**ArI**]$^+$I$^-$ (Figure 3) correspond to monocations. In contrast, the spacings of 0.5 amu observed for the group of peaks at $401 \le m/z \le 407$ point to the presence of a dication (Figure S13, Supporting Information). This assumption was fully born out by fragmentation experiments (Figures S14 and S15, Supporting Information), which moreover permitted its assignment to [L$_2$**Ar**Pd($CH_3CN$)]$^{2+}$. Besides the simple loss of the $CH_3CN$ molecule, eq 6a, the fragmentation involves the exchange of **Ar**$^+$ and Ph groups, eq 6b.[25]

$$[L_2\mathbf{Ar}Pd(CH_3CN)]^{2+} \rightarrow [L_2\mathbf{Ar}Pd]^{2+} + CH_3CN \quad (6a)$$

$$\rightarrow [(\mathbf{Ar}PPh_2)Pd]^+ + [PPh_4]^+ + CH_3CN \quad (6b)$$

The [L$_2$**Ar**Pd($CH_3CN$)]$^{2+}$ ($m/z$ 403) dication apparently originated from [L$_2$**Ar**PdI]$^+$ ($m/z$ 892) by dissociation of I$^-$ and addition of one solvent molecule. Again, the observed behavior matches the generally accepted mechanism depicted in Scheme 1. This agreement gives us additional confidence in the validity of our approach.

We also briefly investigated the reaction of Pd($PPh_3$)$_4$ with the charge-tagged alkyl iodide [**RI**]$^+$I$^-$ in $CH_3CN$. Under similar conditions, [**RI**]$^+$I$^-$ yielded significantly less insertion product (Figure S16, Supporting Information) than [**ArI**]$^+$I$^-$. This finding is in accordance with the well-known lower tendency of alkyl halides toward oxidative addition to Pd(0) compared to aryl halides.[26] Surprisingly, we consistently found the putative insertion product to contain only oxidized $Ph_3PO$ instead of the original $PPh_3$ ligand. While the presence of small amounts of contaminant $Ph_3PO$ is difficult to exclude and also noticeable in the experiment with [**ArI**]$^+$I$^-$/Pd($PPh_3$)$_4$, it is not clear why it seems to be enriched in the insertion product of the [**RI**]$^+$I$^-$/Pd($PPh_3$)$_4$ reaction. Upon fragmentation, the putative insertion product [(LO)$_2$**R**$^{106}$PdI]$^+$ ($m/z$ 946) exclusively yields [**RI**]$^+$ ($m/z$ 284, Figures S17 and S18, Supporting Information). Given the well-known susceptibility of alkyl palladium species to $\beta$-hydrogen eliminations,[26a,b] the complete absence of such a fragmentation channel is rather unexpected. Thus, we cannot exclude that the putative insertion product ion [(LO)$_2$**R**PdI]$^+$ instead corresponds to the simple adduct [(LO)$_2$Pd(**RI**)]$^+$.

**Organozinc and Organomagnesium Species.** Reaction of Zn dust with the charge-tagged organic iodides [**ArI**]$^+$I$^-$ and [**RI**]$^+$I$^-$ in THF and ESI mass spectrometric analysis of the resulting solutions afforded [**ArH**]$^+$ ($m/z$ 136, Figure S19, Supporting Information) and [**RH**]$^+$ ($m/z$ 158, Figure S20, Supporting Information), thus indicating conversion of both [**ArI**]$^+$ ($m/z$ 262) and [**RI**]$^+$ ($m/z$ 284), but also complete hydrolysis of the charge-tagged organozinc intermediates. A comparison of the two reactions shows complete consumption of the alkyl iodide [**RI**]$^+$ at room temperature overnight, whereas its aryl counterpart [**ArI**]$^+$ did not react

(25) The formation of [$PPh_4$]$^+$ in related gas-phase fragmentations has been reported previously; see ref 17f and Qian, R.; Liao, Y.-X.; Guo, Y.-L.; Guo, H. *J. Am. Soc. Mass Spectrom.* **2006**, *17*, 1582–1589.
(26) (a) Cárdenas, D. J. *Angew. Chem.* **2003**, *115*, 398–401; *Angew. Chem., Int. Ed.* **2003**, *42*, 384−387. (b) Frisch, A. C.; Beller, M. *Angew. Chem.* **2005**, *117*, 680–695; *Angew. Chem., Int. Ed.* **2005**, *44*, 674−688. (c) Ariafard, A.; Li, Z. *Organometallics* **2006**, *25*, 4030–4033.

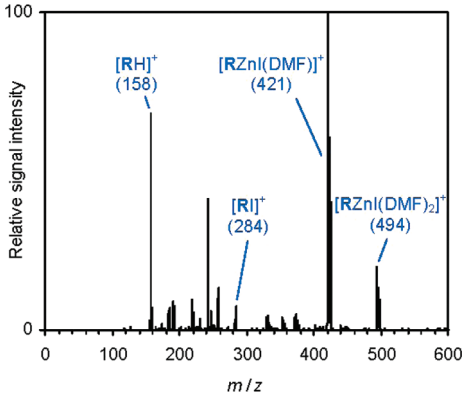


**FIGURE 4.** Positive ion mode ESI mass spectrum of an approximately 1 mM solution of the products ($m/z$ ratios of the most abundant isotopologues in brackets) formed upon reaction of Zn dust with triethyl-(4-iodobutyl)-ammonium iodide ($[\mathbf{RI}]^+I^-$) in DMF measured with the TSQ 7000 instrument. The ion at $m/z$ = 242 corresponds to $Na(DMF)_3^+$, which presumably originates from a contamination of the ESI source.

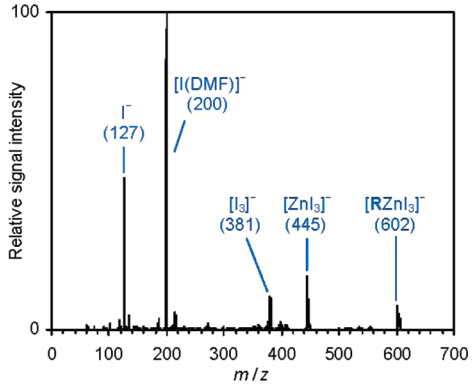


**FIGURE 5.** Negative ion mode ESI mass spectrum of an approximately 1 mM solution of the products ($m/z$ ratios of the most abundant isotopologues in brackets) formed upon reaction of Zn with triethyl-(4-iodobutyl)-ammonium iodide ($[\mathbf{RI}]^+I^-$) in DMF measured with the TSQ 7000 instrument.

to completion even at 50 °C. This lower reactivity of the aryl iodide toward Zn fully agrees with reports in the literature.[27]

The extreme hydrolysis sensitivity of the charge-tagged organozinc intermediates is surprising because previous studies observed related intact zinc species with simple neutral alkyl substituents, such as $[ZnR(THF)_n]^+$ and $[RZnHal_2]^-$ (R = benzyl and butyl, Hal = Br and I, $n$ = 1−3), under very similar experimental conditions.[28,29] The stability of these ions was further enhanced in DMF.[28b] We therefore also tested this solvent for the reaction of Zn with $[\mathbf{RI}]^+I^-$ and now indeed could detect the charge-tagged organozinc species $[\mathbf{R}ZnI(DMF)_n]^+$, $n$ = 1 and 2 ($m/z$ 421 and 494, respectively), along with some hydrolysis product $[\mathbf{RH}]^+$ ($m/z$ 158) and a small amount of remaining reactant $[\mathbf{RI}]^+$ ($m/z$ 284, Figure 4).

The organozinc species observed display the stoichiometry expected for Zn(+2) compounds and moreover provide insight into their solvation behavior. The fact that abundant DMF adducts are found only for Zn-containing species and not for $[\mathbf{RH}]^+$ or $[\mathbf{RI}]^+$ strongly suggests coordination of the solvent molecules to the Zn center and not to the quaternary ammonium group. The inferred coordination numbers of 3 and 4 agree with results obtained for microsolvated alkylzinc cations $[ZnR(solv)_n]^+$ (solv = THF, $CH_3CN$, and DMF), for which coordination numbers ≤4 were observed.[28b,30]

**SCHEME 2. Conceivable Structures for the Observed Anion $[\mathbf{R}ZnI_3]^-$ ($m/z$ 602)**

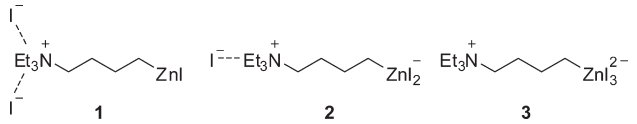


Presumably, these organozinc species adopt tetrahedral coordination geometries[30b] in solution but are prone to lose one solvent molecule during the ESI process. In line with this conjecture, we found mass-selected $[\mathbf{R}ZnI(DMF)_2]^+$ ($m/z$ 494) to lose the attached solvent molecules quite easily when subjected to gas-phase fragmentation (Figure S21, Supporting Information).

The cationic charged tags employed were obviously designed for the detection of organometallic intermediates by positive ion mode ESI mass spectrometry. Therefore, we were surprised that analysis of the products formed upon reaction of Zn with $[\mathbf{RI}]^+I^-$ in DMF by negative ion mode ESI mass spectrometry (Figure 5) resulted in the detection of not only $I(DMF)_n^-$, $n$ = 0 ($m/z$ 127) and 1 ($m/z$ 200), $I_3^-$ ($m/z$ 381), and $ZnI_3^-$ ($m/z$ 445) but also of small quantities of $[\mathbf{R}ZnI_3]^-$ ($m/z$ 602). For the latter, three different structures seem conceivable (Scheme 2).

In structure **1**, two $I^-$ anions are bound electrostatically to the ammonium group. This type of complex is considered less likely because the absence of the analogous ions $[(\mathbf{RH})I_2]^-$ ($m/z$ 412) and $[(\mathbf{RI})I_2]^-$ ($m/z$ 538) in the mass spectrum[31] indicates a low stability of this binding motif under the ESI conditions applied.[32] Structure **2** contains an organozincate moiety, which closely resembles previously observed alkylzincates $[RZnHal_2]^-$.[28] In structure **3**, coordination of all three $I^-$ anions to the Zn atom builds up a 2-fold negative charge at the metal center, which would be prohibitively demanding in energy for a linear conformation.

(27) (a) Knochel, P.; Leuser, H.; Gong, L.-Z.; Perrone, S.; Kneisel, F. F. Polyfunctional Zinc Organometallics for Organic Synthesis. In *Handbook of Functionalized Organometallics*; Knochel, P., Ed.; Wiley-VCH: Weinheim, 2005, Vol. 1, p 251. (b) *Organozinc Reagents*; Knochel, P., Jones, P., Eds.; Oxford University Press: New York, 1999. (c) Krasovskiy, A.; Malakhov, V.; Gavryushin, A.; Knochel, P. *Angew. Chem.* **2006**, *118*, 6186–6190; *Angew. Chem., Int. Ed.* **2006**, *45*, 6040−6044.

(28) (a) Koszinowski, K.; Böhrer, P. *Organometallics* **2009**, *28*, 771–779. (b) Fleckenstein, J. E.; Koszinowski, K. *Chem.—Eur. J.* **2009**, *15*, 12745–12753.

(29) One may speculate that the long-range electrostatic potential of the charged tag could direct water molecules into the proximity of the Zn−C bond and thus accelerate its protolysis. Note that a similar argument does not hold for the previously observed $[ZnR(THF)_n]^+$ and $[RZnHal_2]^-$ species because their equilibrium concentration is supposedly low in comparison to neutral ZnRHal.

(30) Caggiano, L.; Jackson, R. F. W.; Meijer, A. J. H. M.; Pickup, B. T.; Wilkinson, K. A. *Chem.—Eur. J.* **2008**, *14*, 8798–8802. (b) Dreiocker, F.; Oomens, J.; Meijer, A. J. H. M.; Pickup, B. T.; Jackson, R. F. W.; Schäfer, M. *J. Org. Chem.* **2010**, *75*, 1203–1213.

(31) For the specific experiment shown (Figure 5), analysis of the same sample by positive ion mode ESI mass spectrometry proved the presence of the hydrolysis product $[\mathbf{RH}]^+$ (55% signal intensity relative to that of the base peak $[\mathbf{R}ZnI(DMF)]^+$) and $[\mathbf{RI}]^+$ (10% relative signal intensity).

(32) Note however that the negative ion mode mass spectrum of a solution of pure reactant $[\mathbf{RI}]^+I^-$ in DMF showed small amounts of $[\mathbf{RI}_3]^-$ (Figure S22, Supporting Information), which indicates that coordination of two $I^-$ ions to the quaternary ammonium group can occur.

However, adoption of a cyclic conformation could permit a stabilizing electrostatic interaction between the dianionic $ZnI_3$ moiety and the cationic ammonium group. Fragmentation of mass-selected $[\mathbf{R}ZnI_3]^-$ ($m/z$ 602) yields $I^-$ and $[ZnI_3]^-$ as ionic products (Figure S23, Supporting Information), which is of limited significance only because the involvement of rearrangement reactions seems quite likely. Hence, the experimental results do not suffice for an unambiguous structural assignment.

We also attempted the characterization of analogous charge-tagged organomagnesium compounds. However, the very high moisture sensitivity of the intact organomagnesium species precluded their detection. Instead, we only observed degradation products resulting from hydrolysis and/or other decomposition reactions (see Supporting Information for details, including Figures S24−S28).

**Organoindium Species.** Indium powder did not react with the charge-tagged aryl iodide $[\mathbf{Ar}I]^+I^-$ in DMF to a measurable extent. This finding is in line with the previously reported low reactivity of In toward aryl iodides in the absence of LiCl.[33] In contrast, organoindium species did form in the reaction of In with the charge-tagged alkyl iodide $[\mathbf{R}I]^+I^-$ in DMF (Figure S29, Supporting Information) and THF (Figure 6), thus providing rare examples of the insertion of In into a nonactivated carbon−halogen bond.[34] Besides abundant $[\mathbf{R}_2InI_2]^+$ ($m/z$ 683), smaller amounts of $[\mathbf{R}_2InBrI]^+$ ($m/z$ 635/637) were observed. The bromine in the latter originates from the activation of In metal by addition of 1,2-dibromoethane (see Experimental Section). Both complexes are mononuclear and contain In(+3), which indeed is the preferred oxidation state in organoindium chemistry.[15] Fragmentation of these species predominantly led to losses of the organyl substituent **R**, eq 7a, and the $NEt_3$ group (Figures S30−S32, Supporting Information). The latter reaction presumably corresponds to a nucleophilic substitution of the ammonium moiety by a halide ion, eq 7b.[35] In addition, the expulsion of EtI occurred to a minor extent, eq 7c.

$$[\mathbf{R}_2InXI]^+ \rightarrow [\mathbf{R}InXI]^+ + \mathbf{R}, \quad X = \text{Br and I} \tag{7a}$$

$$\rightarrow [\mathbf{R}(X(CH_2)_4)InI]^+ + NEt_3, \quad X = \text{Br and I} \tag{7b}$$

$$\rightarrow [\mathbf{R}(Et_2N(CH_2)_4)InX]^+ + EtI, \quad X = \text{Br and I} \tag{7c}$$

For the reactions both in DMF and THF, only small amounts of $[\mathbf{R}H]^+$ ($m/z$ 158) were detected, which reflects the reduced sensitivity of organoindium compounds to hydrolysis.[36] The absence of adducts of $[\mathbf{R}H]^+$ and $[\mathbf{R}I]^+$ with the strong Lewis base DMF (Figure S29, Supporting Information) again indicates a rather low affinity of the quaternary ammonium group to solvation. In turn, the DMF molecule in $[\mathbf{R}InI_2(DMF)]^+$ ($m/z$ 599, for fragmentation experiments, see Figures S33 and S34, Supporting Information) most likely binds to the In atom, thus giving rise to a coordination number of 4. Notably, no DMF adducts of $[\mathbf{R}_2InI_2]^+$ and $[\mathbf{R}_2InBrI]^+$ were observed, suggesting that the metal centers in these complexes are coordinatively saturated. Therefore, these species probably correspond to tetragonal ate complexes (Scheme 3). A completely analogous structure has very recently been proposed for an allylindium species tagged with a phosphonium group (Scheme 3).[14] Apparently, ate complexes are a common motif in organoindium chemistry.

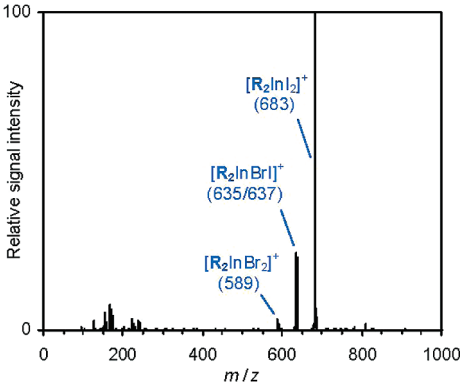


**FIGURE 6.** Positive ion mode ESI mass spectrum of a solution of the products ($m/z$ ratios of the most abundant isotopologues in brackets) formed upon reaction of In with triethyl-(4-iodobutyl)-ammonium iodide ($[\mathbf{R}I]^+I^-$) in THF measured with the TSQ 7000 instrument.

**SCHEME 3. Proposed Organoindium Ate Structures of Charge-Tagged Cations Observed in the Present and Previous Work (X = Br and I)**[14]

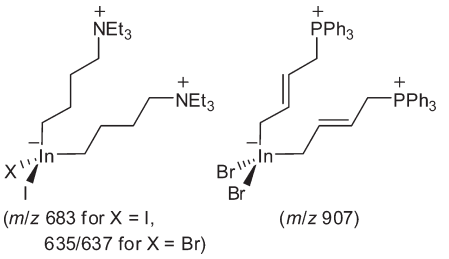


Ate complexes were also observed upon negative ion mode ESI mass spectrometric analysis of the products formed from the reaction of In with $[\mathbf{R}I]^+I^-$ in THF (Figures 7 and S35, Supporting Information). In addition to the purely inorganic $[InI_4]^-$ ion ($m/z$ 623), the organoindium species $[\mathbf{R}InI_4]^-$ ($m/z$ 780), $[\mathbf{R}InBrI_3]^-$ ($m/z$ 732/734, Figure S35, Supporting Information), and $[(I(CH_2)_4InI_3]^-$ ($m/z$ 679) were detected. Upon gas-phase fragmentation, both $[\mathbf{R}InI_4]^-$ ($m/z$ 780, Figures S36−S39, Supporting Information) and $[\mathbf{R}InBrI_3]^-$ ($m/z$ 732/734, Figures S40 and S41, Supporting Information) produce $I^-$ ($m/z$ 127), eq 8a, and in a second major reaction channel, lose EtI, eq 8b. To a much smaller extent, the expulsion of $NEt_3$ was also observed, eq 8c.

$$[\mathbf{R}InXI_3]^- \rightarrow I^- + \mathbf{R}InXI_2, \quad X = \text{Br and I} \tag{8a}$$

$$\rightarrow [(Et_2N(CH_2)_4)InXI_2]^- + EtI, \quad X = \text{Br and I} \tag{8b}$$

$$\rightarrow [(X(CH_2)_4)InI_3]^- + NEt_3, \quad X = I \tag{8c}$$

(33) Chen, Y.-H.; Knochel, P. *Angew. Chem.* **2008**, *120*, 7760–7763; *Angew. Chem., Int. Ed.* **2008**, *47*, 7648−7651.
(34) Yang, Y.-S.; Shen, Z.-L.; Loh, T.-P. *Org. Lett.* **2009**, *11*, 1209–1212.
(35) A somewhat similar nucleophilic substitution has been reported for the gas-phase fragmentations of the adducts of quaternary ammonium cations with a dianion: Gronert, S.; Azebu, J. *Org. Lett.* **1999**, *1*, 503–506.
(36) Li, C.-J.; Chan, T.-H. *Tetrahedron* **1999**, *55*, 11149–11176.

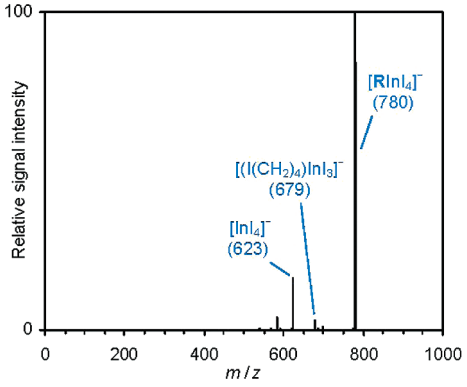


**FIGURE 7.** Negative ion mode ESI mass spectrum of an approximately 2 mM solution of the products (*m*/*z* ratios in brackets) formed upon reaction of In powder with triethyl-(4-iodobutyl)-ammonium iodide ([**R**I]$^+$I$^-$) in THF measured with the HCT ion trap.

**SCHEME 4. Proposed Structures of Charge-Tagged Anions Observed in the Present and Previous Work**[14]

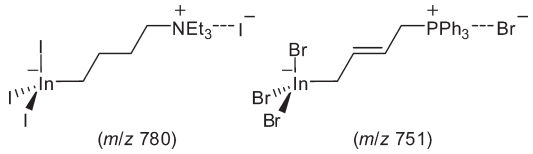


The last two reactions both correspond to nucleophilic substitutions but differ by the position of attack. The preferred pathway involves an attack on the ethyl group, eq 8b, whereas the minor channel proceeds via an attack on the $(CH_2)_4$ linker, eq 8c. Interestingly, this partitioning seems to be just reversed in comparison to the fragmentation reactions of the [**R**$_2$InXI]$^+$ cations, which strongly favor the loss of $NEt_3$, eq 7b, over that of EtI, eq 7c. The deviating reactivity patterns probably reflect structural differences: Unlike [**R**$_2$InXI]$^+$, the [**R**InI$_4$]$^-$ complex, as well as its [**R**InBrI$_3$]$^-$ analogue, contains one iodide ion more than needed for a tetragonal coordination of the In center. Most likely, this additional iodide ion interacts with the quaternary ammonium group electrostatically and thus is ideally poised to abstract an ethyl substituent (Scheme 4).[37] Again, a completely analogous structure has been proposed for a related phosphonium-tagged allyl indium anion (Scheme 4).[14]

The [(I(CH$_2$)$_4$InI$_3$]$^-$ ion (*m*/*z* 679) presumably also adopts a tetragonal coordination geometry at the In center. The proposed connectivity of this species is supported by a fragmentation experiment, which results in the loss of HI (Figure S42, Supporting Information). We suggest that the [(I(CH$_2$)$_4$InI$_3$]$^-$ species originates from a nucleophilic substitution of the $NEt_3$ group by an iodide ion in analogy to the corresponding fragmentation of the [**R**$_2$InXI]$^+$ and [**R**InXI$_3$]$^-$ complexes, eqs 7b and 8c, respectively. This substitution may occur already in solution and/or in the gas phase during the ESI process.

**Monitoring of Coupling Reactions.** As shown above, ESI mass spectrometry has permitted us to track the degradation and hydrolysis of organometallics bearing organic substituents with charged tags. Obviously, it would be even more interesting to use this approach for analyzing synthetically valuable reactions of these species. We have done so and demonstrated the potential of this analytical method by studying the Pd-catalyzed cross-coupling of [**Ar**I]$^+$ with benzylzinc bromide (Negishi cross-coupling), eq 9.

$$[\mathbf{Ar}\mathrm{I}]^+ + \mathrm{BnZnBr} \xrightarrow{[\mathrm{Pd}]} [\mathbf{Ar}\mathrm{Bn}]^+ + \mathrm{ZnBrI} \qquad (9)$$

Negishi cross-couplings constitute one of the most versatile tools in modern organic synthesis.[38] The mechanisms of these reactions therefore have attracted a great deal of attention. It is commonly assumed that these reactions start by the oxidative addition of the organic halide to the zerovalent Pd (or Ni) catalyst. The resulting insertion product then undergoes transmetalation by the organozinc reagent and finally yields the coupling product by reductive elimination.[26b]

For our experiments, we employed Pd(dba)$_2$/tfp (L) in $CH_3CN$ as catalytic system, which efficiently adds [**Ar**I]$^+$ (see above). In the presence of BnZnBr, the expected coupling product [**Ar**Bn]$^+$ (*m*/*z* 226) could indeed be detected by ESI mass spectrometry (Figure 8). The identity of this species was confirmed by analysis of its fragmentation pattern (Figure S43, Supporting Information) and by a control experiment in which BnZnBr was substituted by *m*-methylbenzylzinc bromide. This resulted in a coupling product of an *m*/*z* ratio shifted by 14 amu relative to [**Ar**Bn]$^+$.

In addition, smaller amounts of [L$_2$PdBn]$^+$ (*m*/*z* 661) were produced. Again, this assignment is based on the recorded isotope pattern (Figure S44, Supporting Information), fragmentation experiments (Figures S45 and S46, Supporting Information), and an observed mass shift of 14 amu when BnZnBr was replaced by *m*-methylbenzylzinc bromide. The

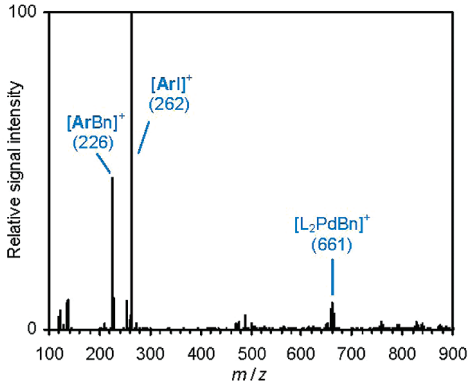


**FIGURE 8.** Positive ion mode ESI mass spectrum of an approximately 2 mM solution of (*p*-iodophenyl)-trimethylammonium iodide ([**Ar**I]$^+$I$^-$), BnZnBr (1.2 equiv), Pd(dba)$_2$ (10 mol %), and tri-(2-furyl)phosphine (L, 20 mol %) in $CH_3CN$ approximately 15 min after mixing measured with the HCT ion trap (*m*/*z* ratios of the most abundant isotopologues of the ions observed given in brackets).

(37) Note that examples of five-fold coordinated In(+3) species are known as well: Yasuda, M.; Haga, M.; Baba, A. *Organometallics* **2009**, *28*, 1998–2000.

(38) (a) Netherton, M. R.; Fu, G. C. *Adv. Synth. Catal.* **2004**, *346*, 1525–1532. (b) Negishi, E.; Hu, Q.; Huang, Z.; Wang, G.; Yin, N. In *The Chemistry of Organozinc Compounds*; Rappoport, Z., Marek, I., Eds.; Wiley: Chichester, 2006; pp 457−553. (c) Organ, M. G.; Avola, S.; Dubovyk, I.; Hadei, N.; Kantchev, E. A. B.; O'Brien, C. J.; Valente, C. *Chem.—Eur. J.* **2006**, *12*, 4749–4755. (d) Manolikakes, G.; Schade, M. A.; Muñoz Hernandez, C.; Mayr, H.; Knochel, P. *Org. Lett.* **2008**, *10*, 2765–2768. (e) Phapale, V. B.; Cárdenas, D. J. *Chem. Soc. Rev.* **2009**, *38*, 1598–1607. (f) Calimsiz, S.; Sayah, M.; Mallik, D.; Organ, M. G. *Angew. Chem.* **2010**, *122*, 2058–2061; *Angew. Chem., Int. Ed.* **2010**, *49*, 2014−2017.

**SCHEME 5. Possible Genesis of the Observed $[L_2PdBn]^+$ Complex (R = 2-furyl)**

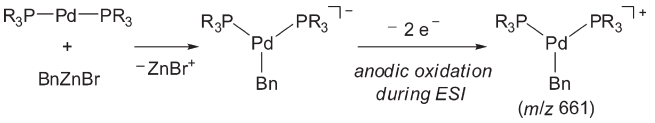


$[L_2PdBn]^+$ ($m/z$ 661) complex accumulated with time and increased in signal intensity as a function of catalyst loading (Figure S47, Supporting Information). Surprisingly, it even formed to some extent in the reaction of the Pd catalyst with BnZnBr in the absence of aryl iodide $[\mathbf{ArI}]^+$ (Figure S48, Supporting Information). However, in this case the abundance of $[L_2PdBn]^+$ ($m/z$ 661) was considerably decreased as indicated by the relatively poor signal/noise ratio. As a consequence, additional ions of similarly low absolute signal intensity, such as $[CuL_n]^+$ and $[(LO)_nZnBn]^+$, also became visible; the assignments of these species, which may have originated from contaminations, are based on the observed isotope patterns and fragmentation experiments (Figures S49−S60, Supporting Information). The genesis of the complex $[L_2PdBn]^+$ ($m/z$ 661) itself is not obvious. The higher absolute signal intensities observed in the presence of added $[\mathbf{ArI}]^+$ might suggest that it forms in a metathesis reaction between the primary insertion product $[L_2\mathbf{Ar}PdI]^+$ and BnZnBr, eq 10.

$$[L_2\mathbf{Ar}PdI]^+ + BnZnBr \rightarrow [L_2PdBn]^+ + [\mathbf{Ar}ZnBr]^+I^- \quad (10)$$

In this case, however, one would also expect to observe $[\mathbf{Ar}ZnX]^+$, X = Br and/or I ($m/z$ 278/280 and 326, respectively, or degradation products thereof), which was not detected. Alternatively, one may speculate that $[L_2PdBn]^+$ ($m/z$ 661) could result from the transmetalation of a Pd(0) species. For related Ni(0) phosphine complexes in the presence of organomagnesium and -zinc reagents, Terao and Kambe have suggested the occurrence of transmetalation reactions and formation of nickelate anions.[39] In analogy, the current experiments might potentially produce a palladate species (Scheme 5). This extremely electron-rich species could then possibly afford the observed $[L_2PdBn]^+$ cation by anodic oxidation during the ESI process.[40] Negative ion mode ESI mass-spectrometric experiments did not detect any palladate species, however, and instead only showed the presence of various zincate complexes (Figure S61, Supporting Information).

Returning to the actual Negishi coupling between $[\mathbf{ArI}]^+I^-$ and BnZnBr itself, we wondered whether ESI mass spectrometry could also be used to monitor the temporal evolution of reactants and products and to derive the rate constant(s) of this reaction. To test for this possibility, we prepared a mixture of the reactants and the catalyst and continuously administered it into the ESI source of the mass spectrometer while recording the positive ion mode ESI mass spectrum. Averaging every 50−100 scans then gave a time resolution of approximately 10 s. The resulting averaged signal intensities still show rather high noise levels (Figure 9), which directly

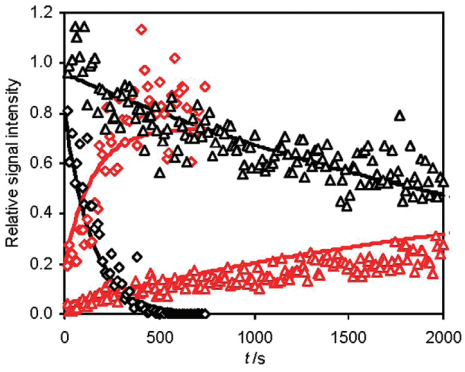


**FIGURE 9.** Time dependence of the normalized signal intensities of reactant $[\mathbf{ArI}]^+$ ($m/z$ 262, black) and product $[\mathbf{Ar}Bn]^+$ ($m/z$ 226, red) formed in the Pd-catalyzed cross-coupling reaction with BnZnBr in $CH_3CN$ at room temperature as determined by ESI mass spectrometry. Results of two experiments with different catalyst loadings are shown (◇ = 100 mol %, △ = 5 mol % relative to $[\mathbf{ArI}]^+$). The solid lines represent simulated time profiles based on a second-order rate constant of $k_2$ = 3.5 L mol$^{-1}$ s$^{-1}$ (see text for details). Time zero corresponds to the start of the ESI mass-spectrometric experiments, which was approximately 2 min after the mixing of the reaction partners.

reflect the relatively poor absolute signal stability typical of the ESI process. Nevertheless, the obtained time profiles clearly exhibit the opposing trends expected for reactants and products. While varying the concentration of the benzylzinc reagent (1.2−2.0 equiv relative to $[\mathbf{ArI}]^+I^-$) did not have a discernible effect, an increase in the catalyst loading strongly accelerated the decay of reactant $[\mathbf{ArI}]^+$ ($m/z$ 262, Figure 9). This finding points to a rate-determining oxidative addition, which is followed by fast transmetalation and reductive elimination steps. The same conclusion can also be derived from the fact that the mass spectra show the simultaneous presence of reactant $[\mathbf{ArI}]^+$ ($m/z$ 262) and product $[\mathbf{Ar}Bn]^+$ ($m/z$ 226) but far less of intermediate $[L_2\mathbf{Ar}PdI]^+$ ($m/z$ 832), because it is almost completely consumed by the fast consecutive reaction with BnZnBr (compare Figure 8, although in this case the lower concentration of the catalyst helps to suppress the relative signal intensity of $[L_2\mathbf{Ar}PdI]^+$). Note that an alternative tagging mode that attached the charged tag to the phosphine ligand would neither permit the detection of the reactant aryl iodide nor the cross-coupling product and thus would be less useful than the present approach.

For a quantitative analysis, we focused on the decline of reactant $[\mathbf{ArI}]^+$ ($m/z$ 262), which according to our model should proceed under pseudo-first-order conditions (virtually constant concentration of free Pd catalyst). Indeed, the individual time profiles of the $[\mathbf{ArI}]^+$ ($m/z$ 262) signal intensity could be satisfactorily fitted with monoexponential functions. Correlating the corresponding pseudo-first-order rate constants with the concentrations of the Pd catalyst in the individual experiments ($c(Pd(dba)_2)$ = $10^{-4}$ to 2 × $10^{-3}$ mol L$^{-1}$) then gave a second-order rate constant of $k_2$ = 4 ± 2 L mol$^{-1}$ s$^{-1}$ for the oxidative addition at room temperature. Based on this value, the decline of the $[\mathbf{ArI}]^+$ ($m/z$ 262) signal intensities in Figure 9 could be reproduced quite well. The derived $k_2$ rate constant was also used to predict the increase of the $[\mathbf{Ar}Bn]^+$ ($m/z$ 226) signal intensities. Here, it

(39) Terao, J.; Kambe, N. *Bull. Chem. Soc. Jpn.* **2006**, *79*, 663–672.
(40) Van Berkel, G. J. *J. Mass Spectrom.* **2000**, *35*, 773–783.

was furthermore necessary to introduce a constant scaling factor to account for apparently slightly deviating ESI response factors[41] of reactant and product ions and/or mass-dependent ion transmission and detection efficiencies. The agreement between observed and simulated signal intensities of the $[\mathbf{ArBn}]^+$ ($m/z$ 226) coupling product does not equal that observed for the $[\mathbf{ArI}]^+$ ($m/z$ 262) reactant but still is reasonably good.

The oxidative addition of $[\mathbf{ArI}]^+$ to $PdL_2$ (L = tfp) in $CH_3CN$ can be compared to the analogous addition of simple PhI to $PdL_2$ in THF and DMF. The latter reactions are somewhat faster ($k_2$(THF) = $500 \pm 200$ and $k_2$(DMF) = $99 \pm 2$ L mol$^{-1}$ s$^{-1}$),[42] although the presence of the electron-withdrawing ammonium group in $[\mathbf{ArI}]^+$ should activate this substrate for the oxidative addition.[43] This comparison suggests that $CH_3CN$ significantly slows down the addition of aryl iodides to zerovalent Pd complexes, presumably by binding to the metal center and blocking of a coordination site. In line with this assessment, $CH_3CN$ is not commonly used as solvent in Negishi cross-coupling reactions,[26b] although its high polarity and volatility make it ideally suitable for the present model studies.

## Conclusions

Zero-valent Pd complexes, Zn, and In react with ammonium-tagged organic iodides under C−I bond insertion. The consumption of the latter can be conveniently monitored by ESI mass spectrometry. In line with well-known reactivity patterns, the Pd complexes preferentially undergo oxidative addition of the aromatic iodide $[\mathbf{ArI}]^+$, whereas Zn and In react more efficiently with the aliphatic iodide $[\mathbf{RI}]^+$. The detection of the resulting organometallic intermediates by ESI mass spectrometry provides detailed information on their molecular nature. In all cases, the stoichiometry of the observed species and the inferred oxidation states of the metal centers are in accordance with the reported chemistry of related systems. This agreement gives us further confidence in the validity of our method. In addition, our findings also provide new insight in that they point to the prominence of ate complexes in organoindium chemistry. This feature has not been fully recognized previously. To a smaller extent, organozinc species apparently form ate complexes as well. While we were unable to detect intact organomagnesium intermediates, we could identify the occurrence of unwanted hydrolysis reactions as the reason for the apparent absence of these species. This information is an important prerequisite for further improving the experimental conditions.

Moreover, the proposed charge-tagging approach also lends itself to reactivity studies. Unlike a tagging scheme that attaches the charge to a coordinating ligand, the placement of the tag in the organyl substituent permits the tracking of the fate of this moiety and thus, e.g., the elucidation of coupling reactions. We demonstrated the feasibility and utility of this approach by analyzing the Pd-catalyzed Negishi cross-coupling of $[\mathbf{ArI}]^+$ with BnZnBr. Our results clearly show that here the oxidative addition is the rate-limiting step, for which we determine a second-order rate constant of $k_2 = 4 \pm 2$ L mol$^{-1}$ s$^{-1}$. Extending this simple and convenient method to the mechanistic analysis of other cross-coupling reactions and different catalytic systems appears straightforward and promising.

## Experimental Section

**Synthesis of Charge-Tagged Precursors.** (*p*-Iodophenyl)-trimethylammonium iodide and (4-iodobutyl)-ammonium iodide were prepared according to known literature procedures.[44]

**Synthesis of Charge-Tagged Organopalladium Species and Sample Preparation.** A dry flask was charged with $Pd(dba)_2$/tfp (2 equiv) or $Pd(PPh_3)_4$, respectively, $[\mathbf{ArI}]^+I^-$ or $[\mathbf{RI}]^+I^-$ (1 equiv), respectively, and $CH_3CN$ under argon atmosphere. After the resulting solution ($c \approx 2$ mM) had stirred for 1−5 h at room temperature, an aliquot was taken and diluted with $CH_3CN$ to the desired concentration.

**Synthesis of Charge-Tagged Organozinc Species and Sample Preparation.** A flask was flame-dried under high vacuum and allowed to cool under argon atmosphere. The procedure was repeated twice, and Zn dust (1.4 mmol) and 1 mL of solvent (THF, freshly distilled from sodium benzophenone ketyl, or DMF, stored over molecular sieves) were added. The Zn metal was activated by the addition of 1,2-dibromoethane (4 $\mu$L) and TMSCl (4 $\mu$L) followed by a short boiling-up of the suspension. Next, 0.7 equiv of $[\mathbf{ArI}]^+I^-$ or $[\mathbf{RI}]^+I^-$, respectively, was added, and the resulting suspension was stirred for 14 h at room temperature or at 50 °C. Solid material remaining was allowed to settle down before an aliquot of the supernatant solution was diluted with the respective solvent.

**Synthesis of Charge-Tagged Organomagnesium Species and Sample Preparation.** A flask was flame-dried under high vacuum and allowed to cool under argon atmosphere. The procedure was repeated twice, and Mg turnings (2.0 mmol) and 2 mL of THF (freshly distilled from sodium benzophenone ketyl) were added. The Mg metal was activated by the addition of $i$Bu$_2$AlH (1 $\mu$L), and the suspension was stirred for 5 min at room temperature. Next, 0.5 equiv of $[\mathbf{ArI}]^+I^-$ or $[\mathbf{RI}]^+I^-$, respectively, was added, and the resulting suspension was stirred for 14 h at room temperature or at 50 °C. Solid material remaining was allowed to settle down before an aliquot of the supernatant solution was diluted with THF.

**Synthesis of Charge-Tagged Organoindium Species and Sample Preparation.** A flask was flame-dried under high vacuum and allowed to cool under argon atmosphere. The procedure was repeated twice, and In powder (0.5 mmol) and 2 mL of solvent (THF, freshly distilled from sodium benzophenone ketyl, or DMF, stored over molecular sieves) were added. The In metal was typically activated by the addition of 1,2-dibromoethane (3 $\mu$L) followed by a short boiling-up of the suspension. Next, 0.7 equiv of $[\mathbf{ArI}]^+I^-$ or $[\mathbf{RI}]^+I^-$, respectively, was added (in the case of THF, only 0.35 equiv was added because of the relatively poor solubility of $[\mathbf{ArI}]^+I^-$ and $[\mathbf{RI}]^+I^-$ in this solvent) and the resulting suspension was stirred for 2−24 h at room temperature. Solid material remaining was allowed to settle down before an aliquot of the supernatant solution was diluted with the respective solvent.

**Sample Preparation for Negishi Cross-Coupling Experiments.** A flame-dried flask was charged with $[\mathbf{ArI}]^+I^-$ and $CH_3CN$ (dried over molecular sieves) under argon atmosphere. To the resulting 2 mM solution were added BnZnBr or *m*-methylbenzylzinc bromide (1.2 or 2.0 equiv, $c \approx 0.85$ M, in THF),[45]

(41) (a) Tang, L.; Kebarle, P. *Anal. Chem.* **1993**, *65*, 3654–3668. (b) Enke, C. G. *Anal. Chem.* **1997**, *69*, 4885–4893.
(42) Amatore, C.; Jutand, A.; Khalil, F. *Arkivoc* **2006**, 38–48.
(43) (a) Fauvarque, J.-F.; Pflüger, F.; Troupel, M. *J. Organomet. Chem.* **1981**, *208*, 419–427. (b) Jutand, A.; Mosleh, A. *Organometallics* **1995**, *14*, 1810–1817.
(44) (a) Kobayashi, H.; Sonada, T.; Takuma, K.; Honda, N.; Nakata, T. *J. Flourine Chem.* **1985**, *27*, 1–22. (b) Pliml, J.; Borovička, M.; Protiva, M. *Collect. Czech. Chem. Commun.* **1958**, *23*, 704–711.
(45) The organozinc reagents were prepared according to a procedure reported in the literature: Berk, S. C.; Yeh, M. C. P.; Jeong, N.; Knochel, P. *Organometallics* **1990**, *9*, 3053–3064.

respectively, and $Pd(dba)_2$/2 tfp (0.05, 0.10, or 1.0 equiv) at −20 °C. After mixing, an aliquot of the undiluted solution was taken, warmed to room temperature, and immediately analyzed by ESI mass spectrometry.

**ESI Mass Spectrometric Experiments.** Sample solutions were transferred into a gastight syringe and administered into the ESI source of a mass spectrometer at flow rates of approximately 5−30 $\mu$L min$^{-1}$. Most of the experiments were performed with a TSQ 7000 multistage mass spectrometer (Thermo MAT), which has been described in more detail before.[46] Nitrogen was used as sheath gas, and ESI voltages ranging from 3.0 to 4.5 kV were applied. Relatively gentle ESI conditions were chosen, the heated capillary being held at 60−100 °C. The $m/z$ ratios of the ions were then determined by scanning the first quadrupole mass filter. For the gas-phase fragmentation experiments, the first quadrupole mass filter was used to mass-select the ions of interest, which then passed an 18 cm long octopole ion guide filled with argon (Linde, 99.998% purity, $p$(Ar) = 0.6−0.9 mtorr as measured with a Convectron). The collision energy $E_{LAB}$ was controlled by adjusting the voltage offset of the octopole. The $m/z$ ratios of the fragment ions were then determined by scanning the second quadrupole mass filter before the ions reached the detector.

The experiments probing the cross-coupling reaction of $[\mathbf{ArI}]^+$ with benzylzinc bromide were performed with a HCT quadrupole ion trap (Bruker Daltonik). Nitrogen was used as sheath gas and an ESI voltage of 3.5 kV was applied. Standard ESI conditions were chosen with nitrogen heated to 60 °C employed as drying gas (5.0 L min$^{-1}$). The ions were then transferred into the instrument's three-dimensional quadrupole ion trap filled with helium (Air Liquide, 99.999% purity, estimated pressure $p$(He) ≈ 2 mtorr). The Compass 1.3 software package was used to eject the ions from the trap for their detection. Similar settings were also used for probing the charge-tagged intermediates formed in the reactions of $[\mathbf{ArI}]^+$ with $Pd(dba)_2$/tfp. In this case, fragmentation was achieved by subjecting the mass-selected ions to excitation voltages of amplitudes $V_{exc}$ and allowing them to collide with He gas.

(46) Koszinowski, K.; Böhrer, P. *Organometallics* **2009**, *28*, 100–110.

**Acknowledgment.** We thank the Deutsche Forschungsgemeinschaft (SFB 749) and the Fonds der Chemischen Industrie for financial support. We also thank Chemetall GmbH (Frankfurt), Evonik Industries AG (Hanau), and BASF AG (Ludwigshafen) for generous gifts of chemicals. M.A.S. and P.K. gratefully acknowledge funding by the European Research Council. J.E.F. and K.K. thank Prof. Herbert Mayr for his continuous generous support and the Munich Center for Integrated Protein Science CIPS$^M$ for additional funding.

**Supporting Information Available:** Additional ESI mass spectra and a more detailed description of the experiments aiming at the detection of charge-tagged organomagnesium species. This material is available free of charge via the Internet at http://pubs.acs.org.